International Journal of Nanomedicine

Dovepress
Taylor & Francis Group

Open Access Full Text Article

ORIGINAL RESEARCH

Targeted Glioma Therapy via TMVP1 Peptide-Modified FLT4 Liposomes: A Novel Molecular Probe Strategy

Yuzhu Zhou[1,2,*], Liwen Chen[1,2,*], Chao Shang[1,*], Yang Hong[2], Hui Zhang[3]

[1]Department of Neurobiology, School of Life Sciences, China Medical University, Shenyang, Liaoning, 110022, People's Republic of China; [2]Department of Neurosurgery, Shengjing Hospital, China Medical University, Shenyang, Liaoning, People's Republic of China; [3]Department of Urology, Shengjing Hospital, China Medical University, Shenyang, Liaoning, People's Republic of China

*These authors contributed equally to this work

Correspondence: Yang Hong, Department of Neurosurgery, Shengjing Hospital, China Medical University, Shenyang, Liaoning, People's Republic of China, Email hongy@sj-hospital.org; Hui Zhang, Department of Urology, Shengjing Hospital, China Medical University, Shenyang, Liaoning, People's Republic of China, Tel/Fax +86-24-31927903, Email zhangh10@sj-hospital.org

Introduction: Glioma is the most common primary malignant tumor in the brain, characterized by rapid growth, strong invasiveness, and unclear lesion boundaries. Current drug treatments have the problems of weak targeting and poor therapeutic effect. TMVP1 is a tumor-targeting peptide that specifically binds to FLT4, a receptor involved in glioma angiogenesis. Its high affinity and selectivity for FLT4 make it an ideal candidate for targeted drug delivery. By functionalizing TMZ-loaded liposomes with TMVP1 (TMZ@Lip-TMVP1), we aimed to enhance glioma-specific targeting and therapeutic efficacy.

Methods: FLT4 was validated as a therapeutic target for glioma by bioinformatics analysis, RT-qPCR, and immunofluorescence experiments. The targeting ability of TMVP1 to FLT4 was confirmed using colocalization and surface plasmon resonance (SPR) experiments. The physicochemical properties of TMZ@Lip-TMVP1, including potential, particle size, TMZ encapsulation efficiency, and peptide coupling rate, were characterized. In vitro cytotoxicity tests were performed to evaluate biocompatibility and therapeutic efficacy. In addition, the targeted delivery and therapeutic impact of TMZ@Lip-TMVP1 were evaluated in subcutaneous tumor-bearing nude mice.

Results: Based on bioinformatics, RT-qPCR, and immunofluorescence results, FLT4 was identified as a reliable therapeutic target for glioma. Colocalization and SPR experiments showed that TMVP1 could effectively bind to FLT4. TMZ@Lip-TMVP1 had good stability and physicochemical properties. Cytotoxicity experiments showed that liposome microcapsules had good biocompatibility, and TMZ@Lip-TMVP1 significantly enhanced the killing effect on glioma cells compared with unmodified liposomes. In vivo experiments showed that TMZ@Lip-TMVP1 could effectively target FLT4 and improve the therapeutic effect of glioma mouse models.

Discussion: The results confirmed that TMZ@Lip-TMVP1 can efficiently deliver TMZ to glioma cells by targeting FLT4, improving the therapeutic effect. This targeted delivery platform provides a promising approach for glioma treatment. In addition, the modular nature of this molecular probe system allows functional adjustment by modifying the coating material, which may enable wider applications in targeted drug delivery and precision medicine.

Keywords: glioma, FLT4, TMVP1 peptide, temozolomide, tumor homing peptide

Introduction

Gliomas originate from the transformation of glial cells and are the most common primary malignant tumors in the brain.[1] Glioma cells often grow along nerve fibers and spread to surrounding brain regions, exhibiting strong invasiveness. This characteristic blurs the boundaries between tumor tissue and adjacent healthy tissue, making it difficult to completely remove the tumor through surgery.[2–4] As research on gliomas has progressed, molecular

Received: 13 January 2025
Accepted: 16 April 2025
Published: 23 April 2025

therapy has gradually become crucial, with a particular focus on the study of biomarkers and molecular targets, leading to the accumulation of extensive diagnostic experience.[5,6] Molecular probes are commonly used markers in molecular therapy, capable of specifically targeting and binding to cells or cellular structures.[7,8] These probes typically consist of functional elements, linking fragments, and recognition components, with the recognition portion being the core. Once the probe reaches the target area, it achieves targeted treatment or diagnosis through specific binding.[9–12]

Fms-like tyrosine kinase 4 (FLT4), also known as vascular endothelial growth factor receptor 3 (VEGFR3), is a tyrosine kinase receptor for VEGF-C and VEGF-D, and has been shown to play a critical role in tumor metastasis and invasion.[13] In recent years, multiple studies have indicated that FLT4 plays a crucial role in the formation and maintenance of tumor-associated lymphatic vessels in gliomas, and is closely related to tumor proliferation, invasion, and metastasis, making it one of the key biomarkers for gliomas.[14] FLT4 expression is significantly elevated in the lymph nodes surrounding glioma and in areas where lymphatic vessels form. Moreover, FLT4 expression varies across different grades of gliomas, and it can specifically bind with the targeted peptide TMVP1, suggesting that FLT4 is a promising target for glioma therapy.

Homologous peptides are a class of peptides capable of specifically targeting tumor tissues or blood vessels.[15,16] They can recognize and bind to specific receptors or biomarkers on the surface of tumor cells, enabling the precise delivery of drugs or imaging agents, thereby reducing non-targeted distribution and toxicity to normal tissues. Phage display peptide libraries(PDPL) are commonly used to screen these target-specific peptide sequences.[16,17] TMVP1 is a novel tumor-targeting peptide screened from PDPL. Its core sequence LARGR has the ability to specifically recognize FLT4.[18] TMVP1 improves its affinity for FLT4 through a cyclized structure, and has a faster binding speed and lower immunogenicity than traditional monoclonal antibodies, thereby achieving more precise targeting.[19] In tumor-targeted drug delivery, TMVP1 can promote the enrichment of drugs in FLT4 high-expression areas and enhance anti-tumor effects. It provides a new method for the design of glioma molecular probes. Temozolomide(TMZ) is a novel oral alkylating anticancer drug with broad-spectrum antitumor activity.[20,21] It can cross the blood-brain barrier,[22] has high bioavailability, effectively extends patient survival, and has high safety and low side effects, making it the first-line drug for the treatment of gliomas internationally.[23]

In conclusion, FLT4 is a reliable target for gliomas, and TMVP1, as a targeting peptide, can specifically bind to FLT4. By combining both to form a molecular probe, we can carry TMZ to evaluate its function in vitro and conduct treatments in mouse models. If the results are favorable, a viable molecular probe for the diagnosis and treatment of gliomas can be developed. This study hypothesizes that the targeting peptide TMVP1 can stably bind to glioma cells in vitro, with potential for imaging and targeted therapy. Ultimately, a molecular probe platform targeting FLT4 using TMVP1 could be established, enabling the delivery of imaging agents, contrast agents, or drugs, thereby achieving precise diagnosis and treatment of gliomas.

Materials and Methods

Experimental Preparation

Bioinformatics Data Collection

Glioma transcriptome data and relevant clinical data were collected from the TCGA database, including 153 high-grade glioma(HGG) transcriptome data samples and 513 low-grade glioma(LGG) transcriptome data samples.[24] Additionally, 2647 HGG cancer-adjacent tissue clinical samples and 2642 LGG cancer-adjacent tissue clinical sample information were obtained from GTEx.[25]

Synthesis of TMZ Liposomes

Using an electronic balance, accurately weigh 8 mg of TMZ and dissolve it in 1 mL of methanol, 100 mg of EPC, 20 mg of cholesterol, and 20 mg of DSPE-mPEG. Dissolve it in 4 mL of chloroform solution using ultrasound and prepare liposome microcapsules using the thin film dispersion method. We successfully produced 10 mL TMZ@Lip-TMVP1 and 10 mL TMZ@Lip Solution.

Tissue Sample Collection

Glioma samples and normal brain tissues were obtained from inpatients at the Department of Neurosurgery, Shengjing Hospital of China Medical University (Shenyang, China), including 4 normal brain tissues, 8 LGG tissues, and 16 HGG tissues. The study protocol was approved by the Ethics Committee of Shengjing Hospital (Approval number: 2021PS778K), and all patients were informed about the use of their tissues and signed informed consent forms. Postoperative tissues were stored in liquid nitrogen. And this study complies with the Declaration of Helsinki.

Preparation of Human Glioma Cell Lines

HEB cells were purchased from Fenghui Biotechnology (Hunan, China). U87 and U251 cells were purchased from Cell Resource Center, Institute of Basic Medical Sciences, Chinese Academy of Medical Sciences. U373 cells were purchased from Thermo Fisher Scientific (USA). DMEM high-glucose medium with 10% fetal bovine serum was used for cell culture. The cells were incubated in a constant-temperature cell culture incubator set at 37°C with 5% CO_2.

Experimental Methods

Physicochemical Property Detection of Liposomes

The size and zeta potential of the liposomes were measured using a Malvern dynamic light scattering instrument. The luminescence intensity of the liposomes was tested with a fluorescence spectrophotometer. The morphology of the liposomes was observed using a transmission electron microscope. The TMZ encapsulation rate was detected by high-performance liquid chromatography, and the UV-visible spectrophotometry was used to test the TMVP1 conjugation rate.

Prognosis and Clinical Correlation Analysis of FLT4 Gene Expression

RNAseq data (level 3) and corresponding clinical information of gliomas were obtained from the Cancer Genome Atlas (TCGA) database (https://portal.gdc.com). The Log rank test[26] was utilized to examine the Kaplan-Meier survival analysis and compare the survival disparities between high and low FLT4 expression groups. Additionally, timeROC analysis was conducted to assess the predictive accuracy of the FLT4 gene.

The relationship between FLT4 gene expression and clinical survival was analyzed using the online tool provided by CGGA (http://www.cgga.org.cn/).

For the Kaplan-Meier curve, the p-value, 95% confidence interval, risk ratio (HR), were obtained through the Log rank test and univariate Cox regression.

All analysis methods and R software packages were executed using version 4.0.3 of R software, and a significance level of $p < 0.05$ was considered statistically significant.

RT-qPCR Detection of FLT4 mRNA Expression Differences

Total RNA was extracted from tissue and cell samples using TRIzol (Thermo Fisher Scientific, USA). Subsequently, cDNA was reverse transcribed using the PrimeScript™ RT Reagent Kit (Takara, cat#RR047A, Japan). Then, the TB Green qPCR Detection Reagent Kit (Takara, cat#RR820A, Japan) was used to amplify the FLT4 gene refer to the instructions. The primers were 5′-TCTCAGAGCTCAGAAGAGG-3′ (forward) and 5′-CAGTTGTAATACCTGGCGG-3′ (reverse). The relative expression level of FLT4 was calculated using the $2^{-\Delta\Delta CT}$ method after normalization with the internal reference gene (GAPDH).

Immunofluorescence

Take 100 μL of cell suspension with good morphology and in logarithmic growth phase and place it in the center of the fluorescent dish. After fixing, permeabilizing and blocking the cells, incubate them with FLT4 antibody (Boster Biotechnology) and DAPI overnight. Take pictures with a laser confocal microscope (Nikon, Japan) and observe the cells under a 60x oil lens. After the experiment, use ImageJ software to process the images.

Fluorescence Peptide in vitro Binding Experiment

Add 10 mg of FAM-labeled TMVP1 powder to 2 mL of sterile PBS solution and mix well. After washing the cells in the fluorescent dish, add 100 μL of TMVP1 solution, FLT4 antibody and DAPI for incubation and staining. Take pictures with a confocal ARX microscope (Nikon, Japan), observe the cells under a 60x oil lens, and process the images with ImageJ software.

Cytotoxicity Assay

The CCK-8 method was used for the cell toxicity experiment. Additionally, a TMVP1 group was set up to verify the biological toxicity of pure TMVP1 peptide. The concentration gradient was 0, 15, 30, 60, 120 μg/mL, mixed with culture medium containing 10% serum, and 100 μL was added per well. The blank group received an equal amount of culture medium. Since the experimental group's drug was labeled with fluorescence, a control group was added for each experiment, replacing the CCK-8 reagent with an equal amount of culture medium, and the D (450) control group was measured. The D (450) experimental group was then calculated by subtracting the D (450) control group from the previously measured D (450).

Cell viability (%) = [D (450) experimental group − D (450) blank group]/[D (450) control group − D (450) blank group] × 100%.

Surface Plasmon Resonance (SPR) Experiment

Considering the small molecular weight and short peptide chain of TMVP1, SPR experiments were chosen to verify the binding of FLT4 with TMVP1. A total of 300 μL of TMVP1 solution at a concentration of 10 mg/mL was used as the analyte in the mobile phase, and 100 μL of FLT4 protein at a concentration of 0.6 mg/mL was directly coupled to the CM5 chip surface using the ForteBio Octet96e instrument for SPR experiments. The experimental results were analyzed and processed using BLAevaluation software (Version 3.1).

Treatment of Subcutaneous Tumors in vivo

Twenty-four 4-week-old BALB/C-nude mice were purchased, including 12 females and 12 males (purchased from Beijing Huafukang Biotechnology Co., Ltd., China), and were raised in the SPF-level Experimental Animal Center of Shenbei Campus of China Medical University. All animal operations were performed in accordance with the regulations approved by the Animal Experimental Center of China Medical University and the Animal Care and Use Committee of China Medical University (ethical approval number: CMU20231381). Human glioma U87MG cell line was used for subcutaneous tumorigenesis. Use a 1 mL sterile syringe to inject 1×10^6 U87MG cells in the logarithmic growth phase into the right axilla of the mouse. After about a week, tumors began to grow under the mice's skin. Mice of the same sex were divided into three groups and administered via tail vein injection. Control group: 0.2 mL normal saline; Experimental group A: 0.2 mL TMZ@Lip solution with a concentration of 30 μg/mL; Experimental group B: 0.2 mL TMZ@Lip-TMVP1 solution with a concentration of 30 μg/mL. Dosage was administered daily and tumor size and mouse growth were recorded. After treatment, all mice were euthanized using a carbon dioxide euthanasia device, and the tumor masses were photographed, removed, and fixed and embedded. Prepare fluorescent stained sections and use a confocal microscope to capture images with excitation light of 488 nm and emission light of 530 nm.

Statistical Methods

Based on the expression data of glioma and normal brain tissue from the CGGA database and TCGA database, a meta-analysis of FLT4 was conducted using STATA (version 17.0) software.

All experiments were independently repeated three times, and the data are presented as the mean ± standard deviation. For multiple groups, the statistical software SPSS 19.0 was utilized to conduct *t*-tests for pairwise comparisons, and one-way ANOVA was employed to analyze differences between groups. A p-value less than 0.05 was deemed statistically significant.

Experimental Results

FLT4 Expression Analysis and Prognosis Analysis in Glioma

To confirm the high expression of FLT4 in tumor tissues, we analyzed the TCGA and GTEx databases. The results showed that FLT4 was significantly overexpressed in gliomas. The average expression level of the GBM group was higher than that of the LGG group (Figure 1A, $P<0.001$). The expression of FLT4 in the glioma group was significantly higher than that of normal tissue. The expression of FLT4 in GBM group was higher than that in LGG group ($P<0.001$).

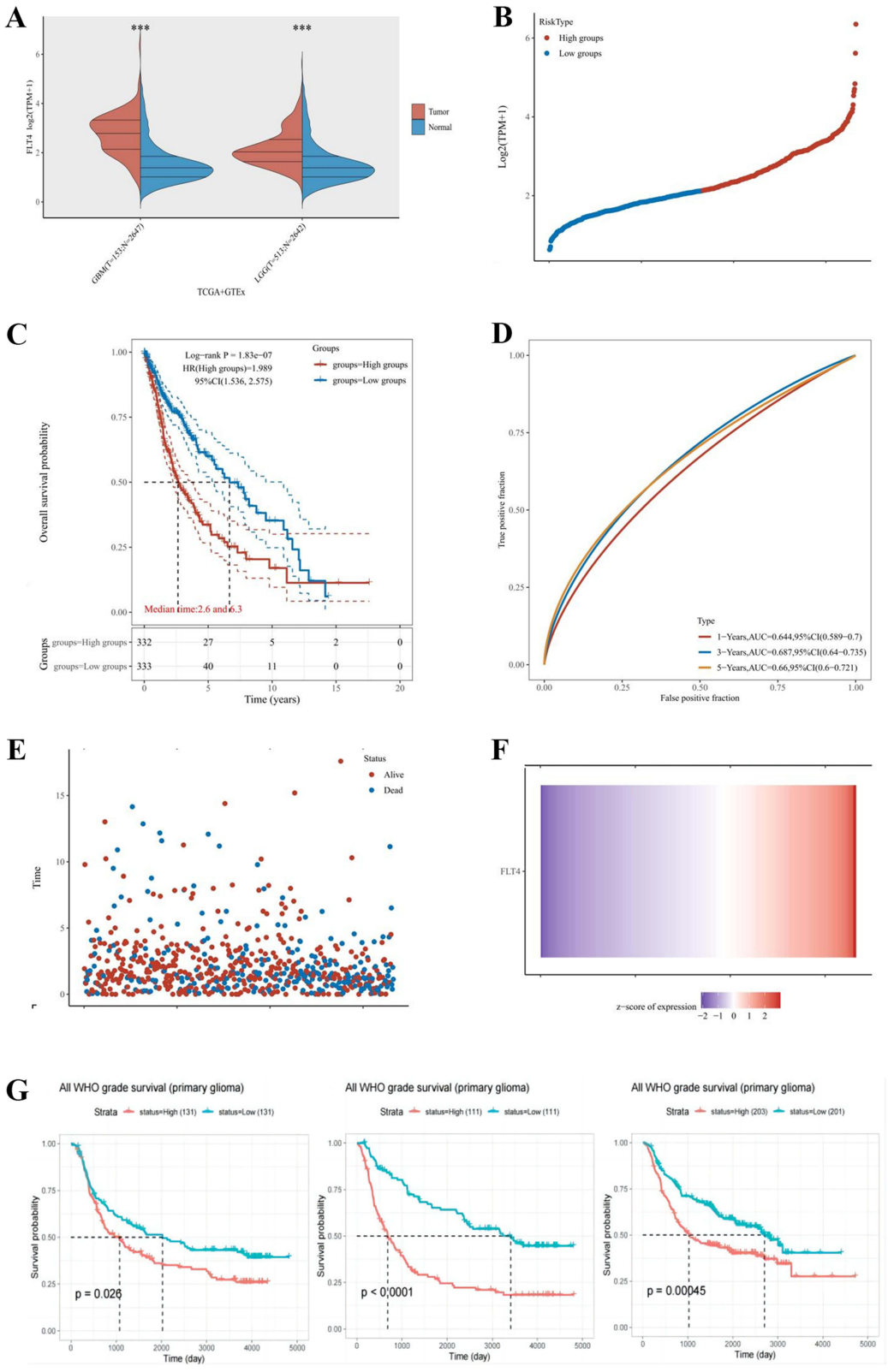

Figure 1 Bioinformatics Analysis of FLT4. (**A**) FLT4 expression analysis (*** *P<0.001*). (**B**) Scatter plot of FLT4 gene distribution trend. (**C**) Survival curve based on the TCGA database shows that high expression of FLT4 is a risk factor for glioma, HR=1.989, P<0.0001. (**D**) ROC curve. (**E**) Scatter plot of FLT4 gene expression and survival time. (**F**) Heatmap of FLT4 gene expression. (**G**) Survival analysis of FLT4 in glioma.

https://doi.org/10.2147/IJN.S517222

Next, this study analyzed the TCGA database, showing that FLT4 gene expression increased with tumor grade (Figure 1B). Through Log rank test and single-factor Cox regression analysis, it was found that high expression of FLT4 is a risk factor for glioma, with a risk coefficient HR=1.989 (Figure 1C, $P<0.001$). TimeROC analysis showed that the FLT4 model had moderate prediction accuracy (Figure 1D). In addition, the scatter plot of FLT4 gene expression and survival time showed that increased FLT4 expression levels were associated with a significant increase in patient mortality and shortened survival time (Figure 1E and G). The gene expression heat map showed the expression distribution of FLT4 (Figure 1F). We further analyzed three data sets from CGGA, and the results consistently showed that high FLT4 expression was closely associated with poor prognosis.

Endogenous Expression Verification of FLT4

As shown in Figure 2A, the expression of FLT4 in glioma tissues was significantly higher than that in normal tissues ($P<0.001$), and the expression in the GBM group was significantly higher than that in the LGG group ($P<0.01$), indicating that the expression of FLT4 is closely related to tumors. The degree of malignancy was positively correlated, which was consistent with the results of bioinformatics analysis. Figure 2B shows that the expression levels of FLT4 in the glioma cell lines U373, U251, and U87 are higher than those in the glial cell line HEB ($P<0.05$, $P<0.01$, $P<0.001$). Among various tumor cell lines, the expression of FLT4 in the U87 cell line was significantly higher than that in the U373 cell line ($P<0.01$).

FLT4 Protein Expression Detection and Localization Experiment

The brightness of the blue light channel of the laser confocal microscope was set to 85, and the brightness of the red light channel was set to 110, and the cells were observed under a 60x oil lens. Immunofluorescence results showed that FLT4 protein was mainly localized on the cell membrane. Under the same brightness setting, the red light intensity of glioma cell lines U373 and U87 was significantly higher than that of the glial cell line HEB, indicating that FLT4 protein is highly expressed in glioma cell lines. In addition, among glioma cell lines, the red light intensity of the U87 cell line was higher than that of the U373 cell line, which may be related to the higher malignancy of the U87 cell line (Figure 2C).

Colocalization Detection of TMVP1 and FLT4 Proteins

The blue light channel brightness parameter of the confocal ARX microscope was set to 90, while the green and red light brightness parameters were set to 110. Confocal microscopy imaging revealed that the TMVP1 peptide can colocalize with the FLT4 protein. Similar to the immunofluorescence experiment, the fluorescence intensity in the U87 cell line was higher than in the U373 cell line (Figure 3A). This suggests that the U87 cell line may express more FLT4 protein than the U373 cell line, resulting in a higher binding capacity of the TMVP1 peptide in U87 cells.

Verification of TMVP1 and FLT4 Protein Binding

FLT4 protein, at a concentration of 0.6 mg/mL, was immobilized on the surface of the CM5 chip as the solid phase, while a TMVP1 solution at 10 mg/mL was used as the mobile phase. The ForteBio Octet96e instrument measured the maximum binding response value of the TMVP1 peptide within 150 seconds. The response was quantified in resonance units (RU), where 1 RU corresponds to a 1 pg/mm² change in protein concentration on the CM5 chip surface. At a concentration of 10 mg/mL, the binding response value of TMVP1 to FLT4 protein was 11.5 RU (Figure 3B), indicating a strong binding affinity between the two proteins at this concentration.

Physicochemical Property Detection of TMZ Liposomes

Transmission Electron Microscopy Observation of TMZ Liposomes

The morphology and density of TMZ@Lip-TMVP1 were observed using a transmission electron microscope, showing that the liposome surface was relatively round and the density was relatively uniform (Figure 4A). The scale bar in the figure is 100 nm.

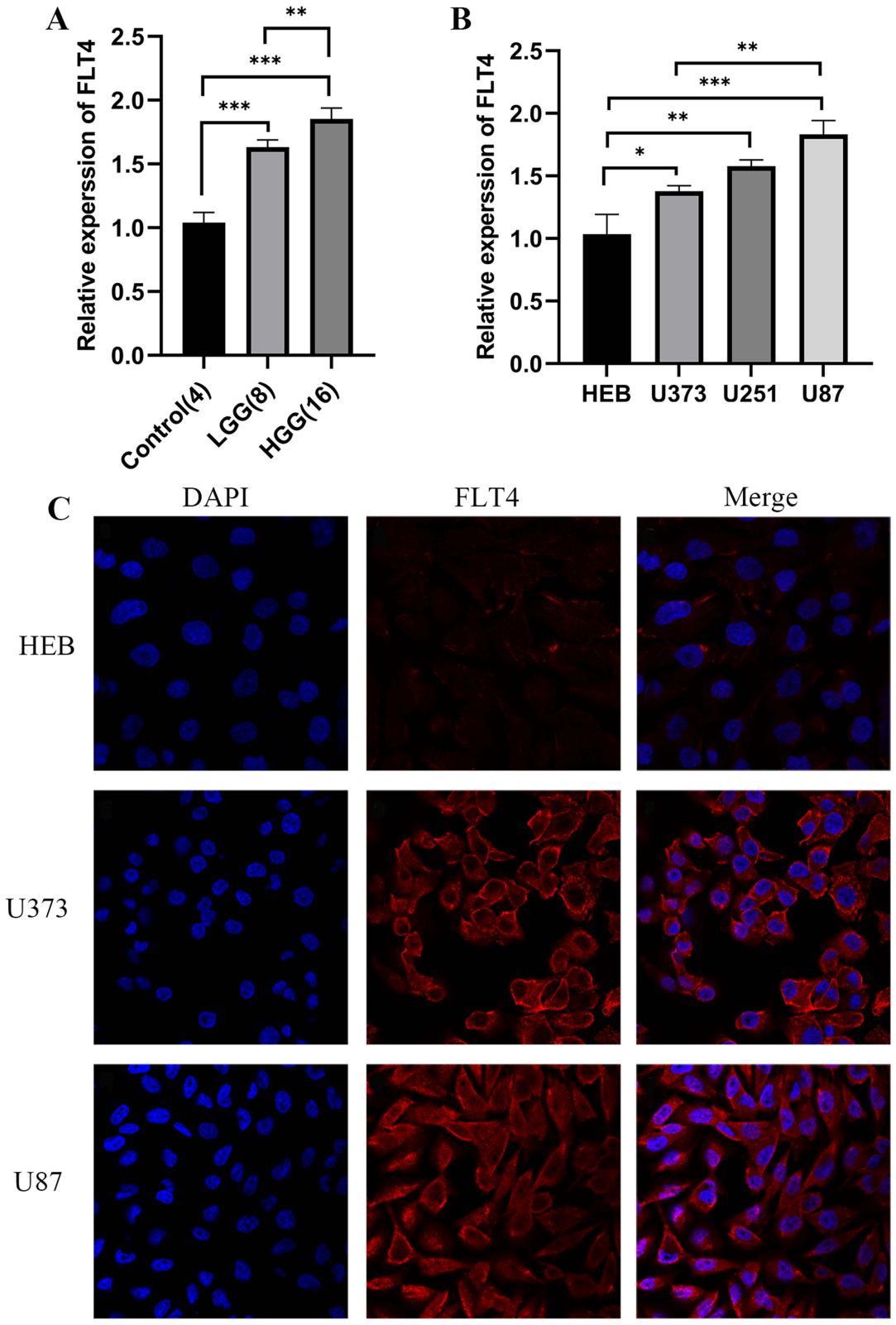

Figure 2 The Expression of FLT4 in Gliomas. (**A**) RT-qPCR detection of expression of FLT4 in glioma tissue (* *P<0.05;* ** *P<0.01;* *** *P<0.001*). (**B**) RT-qPCR detection of expression of FLT4 in glioma cells (* *P<0.05;* ** *P<0.01;* *** *P<0.001*). (**C**) Immunofluorescence images of HEB, U373, and U87 cells.

https://doi.org/10.2147/IJN.S517222

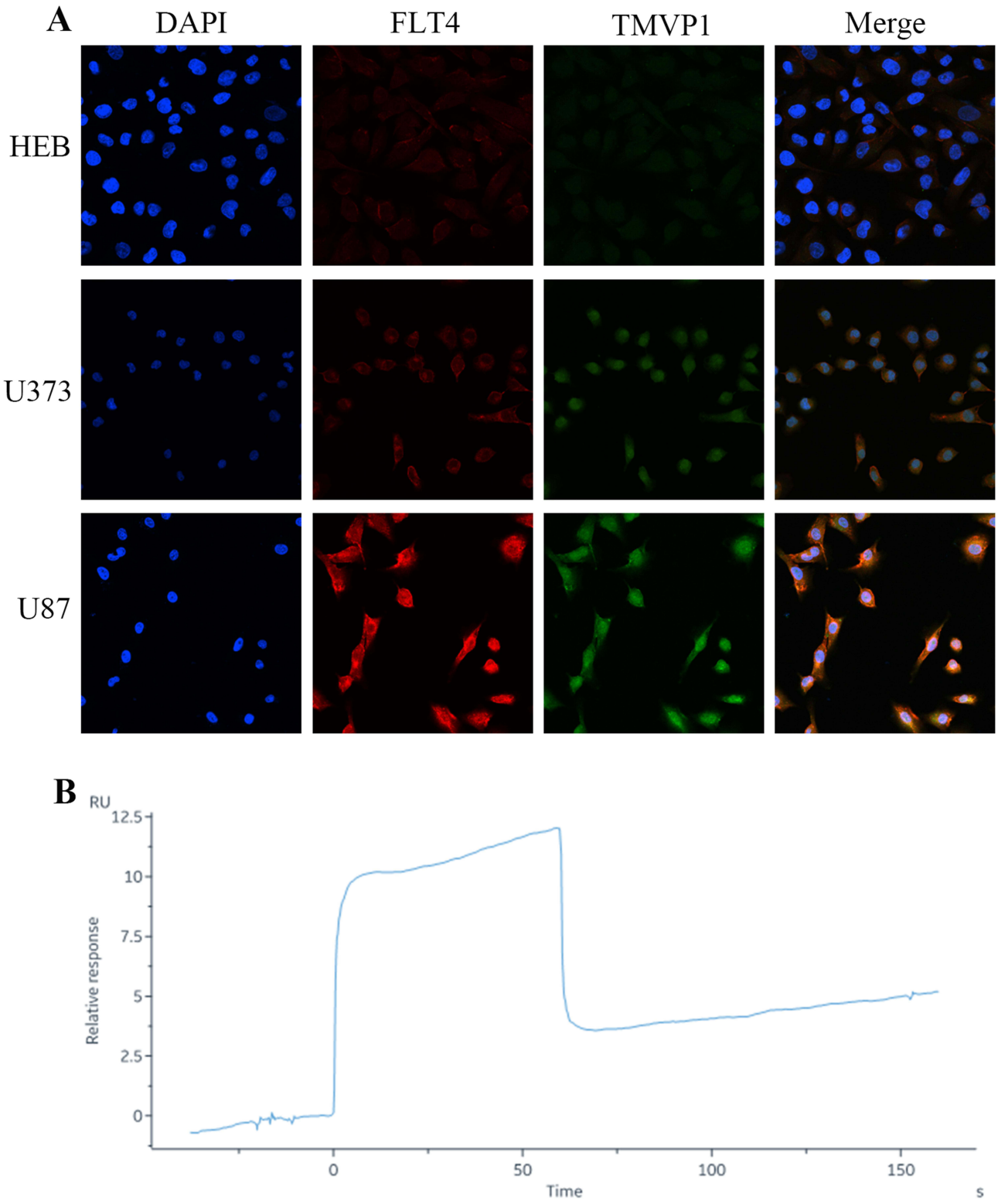

Figure 3 Binding of TMVP1 and FLT4 Proteins. (**A**) Results of in vitro co localization experiment of fluorescent peptides. (**B**) SPR binding curve.

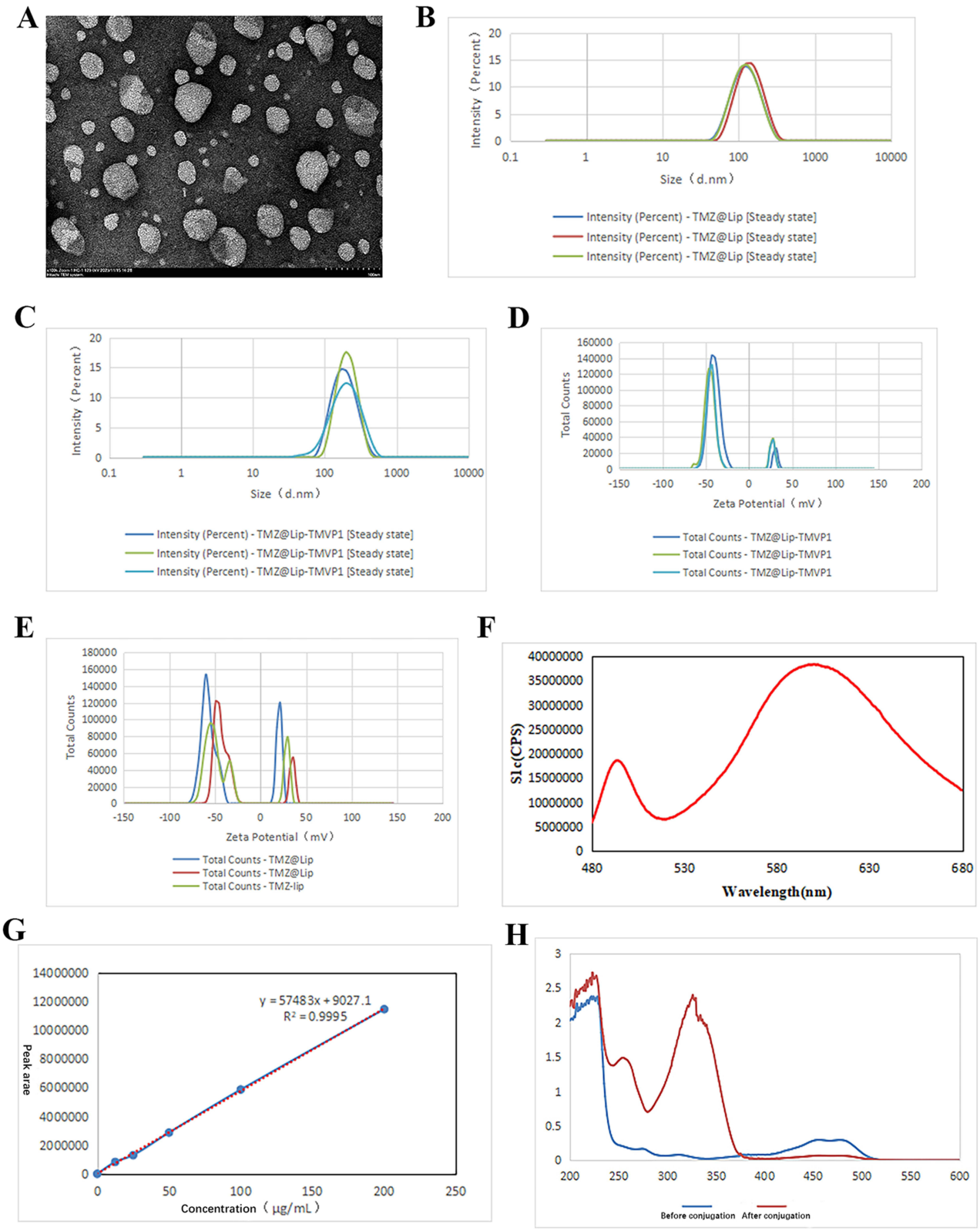

Figure 4 Physical and Chemical Characterization Testing of TMZ@Lip-TMVP1. (**A**) Transmission electron microscopy of TMZ@Lip-TMVP1. (**B**) DLS analysis curve of TMZ@Lip. (**C**) DLS analysis curve of TMZ@Lip-TMVP1. (**D**) Zeta analysis curve of TMZ@Lip-TMVP1. (**E**) Zeta analysis curve of TMZ@Lip. (**F**) Fluorescence spectroscopy of TMZ@Lip-TMVP1. (**G**) Line graph of TMZ concentration and HPLC peak area. (**H**) UV-Visible spectrophotometry test of TMVP1 coupling rate.

https://doi.org/10.2147/IJN.S517222

DLS Detection of Liposome Size

DLS results show that the particle size distribution (Intensity) of TMZ@Lip is 137.6 nm, and the number distribution (Number) is 70.9 nm. After coupling with the peptide TMVP1, the Intensity increased to 207 nm and the Number increased to 122.8 nm (Figure 4B and C). From the data in Table 1, it can be seen that the PDI value of the liposomes after coupling with TMVP1 is lower, indicating that the coupling of TMVP1 makes the particle size distribution of the liposomes more concentrated and the particle size more uniform.

Zeta Detection of TMZ Liposome Potential

Zeta analysis results showed that TMZ@Lip particles were overall negatively charged, with a potential of −32.57 mV, and the potential decreased to −35.39 mV after coupling with TMVP1 (Figure 4D and E, Tables 2 and 3).

TMZ Liposome Fluorescence Spectroscopy Test

Using a fluorescence spectrophotometer, the fluorescence intensity of TMZ@Lip-TMVP1 was tested. The excitation light was set to 468 nm, scanning the emission light spectrum from 480 nm to 680 nm (Figure 4F). The fluorescence intensity peaked at a wavelength of 609 nm, reaching 376224 CPS.

UV-Visible Spectrophotometry Detection of Peptide Coupling Rate

Using the FAM fluorescence-labeled TMVP1, the absorbance at 456 nm was measured using a UV-visible spectrophotometer to calculate the TMVP1 coupling rate as 76.68%, and the peptide TMVP1 concentration was 0.153 mg/mL (Figure 4G).The absorbance before coupling TMVP1 was 0.296, and after coupling, it was 0.069. Therefore, the coupling rate = (absorbance decrease before and after coupling) / (absorbance before coupling) × 100% = 76.68%. Consequently, the TMVP1 concentration can be estimated to be around 0.153 mg/mL.

High-Performance Liquid Chromatography Test for TMZ Encapsulation Efficiency

Using a C18 column, the temperature was set at a constant 30°C. The mobile phase used was methanol: 0.5% acetic acid + H_2O in a ratio of 1:9, and the flow rate was set at 1 mL/min. The injection volume was 20 μL. The wavelength was set to 329 nm. TMZ was prepared in standard solutions with concentration gradients of 12.5, 25, 50, 100, and 200 μg/mL,

Table 1 Sizes of TMZ Liposomes

Samples	Name	Mean	Maximum
TMZ@Lip	Intensity (nm) Number (nm) PDI	137.6 70.9 0.242	147.4 78.48 0.2592
TMZ@Lip-TMVP1	Intensity (nm) Number (nm) PDI	207 122.8 0.1731	212.5 139.9 0.1785

Table 2 TMZ@Lip Zeta Data

Name	Mean	SD	RSD	Minimum	Maximum
Zeta Potential (mV)	−32.57	2.98	9.151	−35.76	−29.86
Conductivity (mS/cm)	0.006002	0	0	0.006002	0.006002
Wall Zeta Potential (mV)	−27.25	7.581	27.82	−35.84	−21.52
Quality Factor	2.061	0.2778	13.48	1.822	2.366
Zeta Peak One Mean	−51.67	7.678	14.86	−58.28	−43.25
Zeta Peak Two Mean	7.135	35.87	502.8	−33.29	35.16

Table 3 TMZ@LP-TMVP1 Zeta Data

Name	Mean	SD	RSD	Minimum	Maximum
Zeta Potential (mV)	−35.39	1.279	3.615	−36.57	−34.03
Conductivity (mS/cm)	0.003228	0	0	0.003228	0.003228
Wall Zeta Potential (mV)	−25.57	1.986	7.766	−26.98	−23.3
Quality Factor	2.307	0.3512	15.22	1.903	2.529
Zeta Peak One Mean	−49.15	12.35	25.13	−63.28	−40.38
Zeta Peak Two Mean	4.029	43.48	1079	−46.12	31.11

and the encapsulation rate of TMZ was determined by measuring the peak area (Table 4). It was found that the increase in chromatographic peak area was linearly related to the increase in TMZ concentration, with a linear regression equation of Y=57483X+9207.1, R^2=0.9995 (Figure 4H). The detection results are as follows: the concentration of TMZ in TMZ@Lip was 420.162 μg/mL, and in TMZ@Lip-TMVP1, it was 408.499 μg/mL. The input amount of TMZ was 8 mg for both, with encapsulation rates of 52.5% and 51.06%, respectively.

Biosafety Testing and in vitro Efficacy Testing of Liposome Microcapsules

The drug and TMVP1 concentration gradients were set at 0, 15, 30, 60, and 120 μg/mL for the cell toxicity test. The CCK-8 assay demonstrated that TMZ@Lip-TMVP1 exhibited stronger cytotoxicity compared to TMZ@Lip and TMZ at concentrations of 30 μg/mL and 60 μg/mL (Figure 5A). In contrast, TMVP1 alone did not show significant cytotoxicity towards U87 cells (Figure 5B). The calculated IC50 value for TMZ@Lip-TMVP1 was 36.36 μg/mL, which was significantly lower than that of the TMZ@Lip control group (48.03 μg/mL) and TMZ (48.43 μg/mL). These results were statistically significant (P<0.0001). Additionally, the CCK-8 assay indicated that the use of liposomes did not affect the efficacy of TMZ itself (P>0.05).

Experimental Study on the Enrichment and Therapeutic Effect of Liposome Microcapsules on Subcutaneous Transplant Tumors

Fourteen days after subcutaneous injection of tumor cells into mice, the tumor diameter on the right side of the mice's armpit measured approximately 0.5 cm (Figure 6A). Treatment began on the 15th day with a daily tail vein injection of 0.2 mL of medication. Prior to treatment, the IC50 values were determined via CCK-8 assays: the IC50 for TMZ@Lip was 48.03 μg/mL, and for TMZ@Lip-TMVP1 was 36.36 μg/mL. To avoid excessive apoptosis, a drug concentration of 30 μg/mL was selected. Tumor size was measured daily, and mouse activity was monitored.

After 15 days of treatment, mice in the control group injected with saline had an average tumor diameter of approximately 1.3 cm (Figure 6B), with skin ulceration covering the tumor and limited movement in the right forelimb.

Table 4 TMZ Concentration and Peak Area

Concentration (μg/mL)	Peak Area
0	0
12.5	827,788
25	1,295,817
50	2,870,482
100	5,869,440
200	11,465,196

https://doi.org/10.2147/IJN.S517222

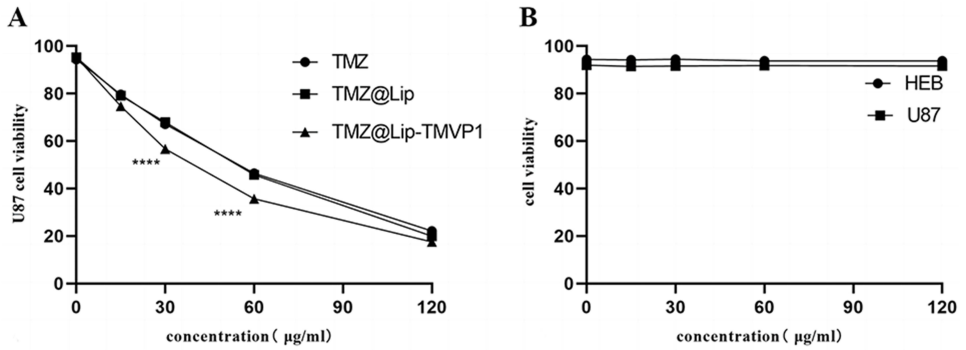

Figure 5 CCK-8 Cell Toxicity Test. (**A**) The TMZ liposome drug cytotoxicity experiment showed that at concentrations of 30 μg/mL and 60 μg/mL, the coupling of TMVP1 could increase the killing power of TMZ@Lip on U87 cells, (**** *P<0.0001*). However, the therapeutic effect of TMZ is not significantly related to whether it is coupled with liposomes, with *P>0.05*. (**B**) The TMVP1 targeting peptide cell toxicity experiment proved that TMVP1 itself had no significant biological toxicity to U87 cells and HEB cells, P>0.05.

Figure 6 Record of Tumor Growth in Nude Mice and Tumor Tissue Collection Photos. (**A**) Tumor longest diameter was about 0.5 cm 14 days after subcutaneous injection of U87 cells. (**B**) Tumor longest diameter was about 1.3 cm after 15 days of injection with saline in the control group. (**C**) Tumor longest diameter was about 1 cm after 15 days of injection with TMZ@Lip in the experimental group. (**D**) Tumor longest diameter was about 0.8 cm after 15 days of injection with TMZ@Lip-TMVP1 in the experimental group. (**E**) Tumor tissue collection from mice, each row from left to right represents the physiological saline group, TMZ@Lip group, and TMZ@Lip-TMVP1 group.

Mice treated with TMZ@Lip showed an average tumor diameter of 1 cm (Figure 6C) and normal limb movement. In contrast, the mice injected with TMZ@Lip-TMVP1 had an average tumor diameter of only 0.8 cm (Figure 6D). Figure 6E shows the comparison of tumor size among different groups of mice. Euthanize the mice the next day using a carbon dioxide euthanasia device. Tumors were then excised, photographed, and fixed in 4% paraformaldehyde. After 24 hours, the samples were paraffin-embedded, sectioned, and observed under a fluorescence microscope

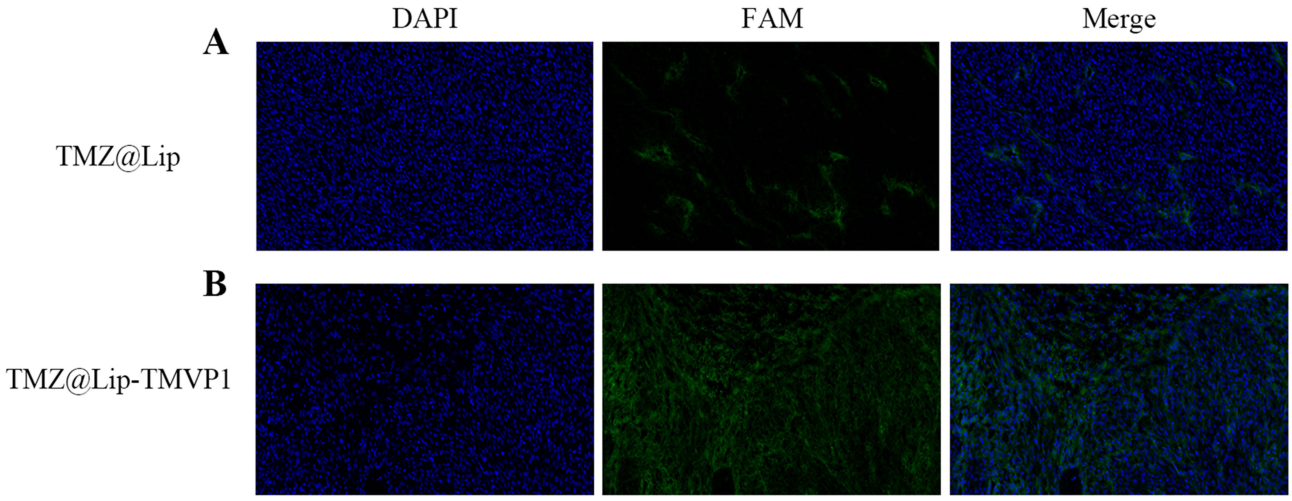

Figure 7 Fluorescence Microscope Photos of Nude Mouse Subcutaneous Transplanted Tumor Slices. (**A**) Fluorescence microscope images of tumor slices from mice treated with TMZ@Lip. (**B**) Fluorescence microscope images of tumor slices from mice treated with TMZ@Lip-TMVP1.

(Figure 7A and B). RGB images of the tumor sections were processed using ImageJ software (version 1.8.0) to isolate the green channel. The average relative fluorescence intensity (FIT) for the TMZ@Lip-TMVP1 group was 15,455 AU, compared to the other groups.

Discussion

Glioblastoma is a highly malignant and invasive primary brain tumor with a poor prognosis.[27] In recent years, studies have found that FLT4 (VEGFR-3) is abnormally highly expressed in a variety of malignant tumors and plays an important role in lymphangiogenesis and tumor microenvironment regulation. Lee et al[28] pointed out that FLT4 plays a significant role in tumor progression, and Mp et al[29] further found that FLT4-targeted nanocarriers can effectively enhance the enrichment of drugs in tumor sites. This study confirmed through bioinformatics analysis, RT-qPCR and immunofluorescence experiments that FLT4 is significantly upregulated in high-grade glioblastoma and is closely associated with poor prognosis (HR = 1.989).[30] This further clarifies the importance of FLT4 as a malignant driver of glioma and a potential therapeutic target, providing new ideas for targeted therapy.[31]

In order to study the binding ability of TMVP1 to FLT4, this study used confocal microscopy and SPR experiments to confirm that TMVP1 has a strong binding affinity with FLT4 (11.5 RU).[32,33] TMVP1 has LARGR as its core sequence, and its ring structure significantly improves its binding stability and reduces the off-target toxicity caused by nonspecific binding. TMVP1 focuses on targeting the transmembrane protein FLT4 and shows significant enrichment ability in GBM, further emphasizing its targeting specificity.[19,34] In addition, TMVP1 shows good biocompatibility and in vivo stability after combining with nanoprobes, significantly reducing off-target toxicity, providing a reliable basis for precision targeted therapy.[35,36] This feature makes TMVP1 more advantageous in FLT4 targeted therapy, especially in the precision treatment of malignant solid tumors such as GBM, and has great application potential.

In this study, by optimizing the liposome coupling strategy, the coupling rate of TMVP1 in the carrier was significantly improved to 76.68%, and the liposome PDI value was lower, the particle size distribution was more uniform, and the stability was higher.[37] Compared with other FLT4 targeting peptides, TMVP1 has obvious advantages in targeting specificity, liposome binding stability and therapeutic effect. The study of Lee et al[28] showed that FLT4 targeting peptides (such as P4 peptide) showed good targeting effect in acute myeloid leukemia. The study of Mp et al[29] optimized FLT4 targeting nanocarriers through PEG surface engineering and improved the aggregation efficiency of drugs on target cells. This study further optimized the TMVP1 conjugation strategy, resulting in a higher TMVP1 conjugation rate, lower liposome PDI value, more uniform particle size, and better stability, which helps penetrate the blood-brain barrier and enhance drug accumulation in the tumor site. Fluorescence imaging results showed that the

https://doi.org/10.2147/IJN.S517222

accumulation of TMZ@Lip-TMVP1 in the tumor site was significantly increased, which was better than other control groups, further demonstrating the advantages of TMVP1 in FLT4 targeted therapy and the potential for precision therapy.[29,38,39]

However, the coupling of TMZ-loaded liposomes with TMVP1 peptides may have a dual effect on blood-brain barrier (BBB) permeability. On one hand, liposome encapsulation can enhance the stability of TMZ in vivo and facilitate its delivery into brain tissue through the transcellular transport mechanism of nanoparticles.[40] On the other hand, if the liposome particle size is too large or surface modifications reduce passive diffusion, TMZ penetration through the BBB may be limited.[41] TMVP1 enhances drug accumulation at tumor sites by specifically binding to FLT4, improving local therapeutic effects. However, if this modification significantly reduces BBB permeability, it could counteract the targeted delivery advantage. Therefore, to verify the feasibility of TMZ@Lip-TMVP1, it is essential to compare the efficacy of free TMZ, TMZ@Lip, and TMZ@Lip-TMVP1 in an intracranial orthotopic glioma model, assessing BBB penetration rate, intratumoral drug enrichment, and therapeutic effects. This will clarify whether TMVP1 modification truly improves targeting without compromising overall drug delivery efficiency. Additionally, future studies should optimize liposome size, surface modifications, and BBB penetration enhancement strategies to achieve the optimal balance between targeted accumulation and efficient BBB penetration, ultimately enhancing precision glioma therapy.[42]

Despite the significant progress achieved in this study, certain limitations remain. For instance, the short fluorescence wavelength resulted in suboptimal in vivo imaging performance. Additionally, TMZ may lead to tumor drug resistance, potentially affecting subsequent therapeutic outcomes.[43,44] Future research should delve deeper into the mechanisms underlying TMZ resistance or explore co-encapsulation of auxiliary drugs alongside TMZ to enhance therapeutic efficacy.[44,45] Furthermore, optimizing the liposome preparation process to improve drug loading efficiency and investigating its potential application in delivering other anticancer drugs could broaden the scope of this platform.[46,47]

In summary, this study provides an innovative strategy for the precision treatment of glioblastoma by constructing a TMVP1-functionalized liposome drug delivery platform and demonstrates its broad potential in future cancer treatment.[19]

Conclusion

This study constructed a TMVP1-modified liposome delivery platform for TMZ, and verified its ability to target glioma tissues and improve the anti-glioma efficiency of TMZ in nude mice with subcutaneous glioma transplants. FLT4 has the potential to be a glioma tumor marker, and TMVP1 specifically binds to FLT4. This study demonstrates the application potential of the TMVP1-modified liposome system, opening up a new direction for the treatment of glioma.

Abbreviations

FLT4, Fms-like tyrosine kinase 4; HGG, high-grade glioma; HR, risk ratio; LGG, low-grade glioma; PDPL, phage display peptide libraries; TCGA, Cancer Genome Atlas; TMZ, Temozolomide; VEGFR3, vascular endothelial growth factor receptor 3.

Data Sharing Statement

The datasets used and analyzed during the current study are available from the corresponding author on reasonable request.

Research Ethics Statement

The study protocol was approved by the Ethics Committee of Shengjing Hospital (Approval number: 2021PS778K), and all patients were informed about the use of their tissues and signed informed consent forms. All animal operations were performed in accordance with the regulations approved by the Animal Experimental Center of China Medical University and the Animal Care and Use Committee of China Medical University (ethical approval number: CMU20231381).

Consent for Publication

The consent for publication were obtained from all patients.

Author Contributions

Yuzhu Zhou: Conceptualization, Investigation, Methodology, Writing - original draft. Liwen Chen: Conceptualization, Investigation, Methodology, Writing - original draft. Chao Shang: Investigation, Methodology, Resources. Yang Hong: Investigation, Data curation, Writing-review and editing, Hui Zhang: Writing-review and editing, Supervision, Funding acquisition. All authors made a significant contribution to the work reported, whether that is in the conception, study design, execution, acquisition of data, analysis and interpretation, or in all these areas; took part in drafting, revising or critically reviewing the article; gave final approval of the version to be published; have agreed on the journal to which the article has been submitted; and agree to be accountable for all aspects of the work. Yuzhu Zhou, Liwen Chen and Chao Shang share first authorship.

Funding

This study was funded by the National Natural Science Foundation of China (No. 81872067) and Liaoning Province Applied Basic Research Plan (2022JH2/101300072).

Disclosure

The authors report no conflicts of interest in this work.

References

1. Zong H, Parada LF, Baker SJ. Cell of origin for malignant gliomas and its implication in therapeutic development. *Cold Spring Harb Perspect Biol*. 2015;7(5):a020610. doi:10.1101/cshperspect.a020610
2. Ghiaseddin AP, Shin D, Melnick K, Tran DD. Tumor Treating Fields in the Management of Patients with Malignant Gliomas. *Curr Treat Options Oncol*. 2020;21(9):76. doi:10.1007/s11864-020-00773-5
3. Azad TD, Duffau H. Limitations of functional neuroimaging for patient selection and surgical planning in glioma surgery. *Neurosurg Focus*. 2020;48(2):E12. doi:10.3171/2019.11.FOCUS19769
4. Niki C, Kumada T, Maruyama T, Tamura M, Kawamata T, Muragaki Y. Primary Cognitive Factors Impaired after Glioma Surgery and Associated Brain Regions. *Behav Neurol*. 2020;2020:7941689. doi:10.1155/2020/7941689
5. Prados MD, Byron SA, Tran NL, et al. Toward precision medicine in glioblastoma: the promise and the challenges. *Neuro Oncol*. 2015;17 (8):1051–1063. doi:10.1093/neuonc/nov031
6. Butowski N. Novel and Prospective Molecular Targets for Therapy of Intracranial Gliomas. *Prog Neurol Surg*. 2018;32:66–78. doi:10.1159/000469681
7. Poletto G, Cecchin D, Bartoletti P, Venturini F, Realdon N, Evangelista L. Radionuclide Delivery Strategies in Tumor Treatment: a Systematic Review. *Curr Issues mol Biol*. 2022;44(8):3267–3282. doi:10.3390/cimb44080225
8. Liu Q, Huang J, He L, Yang X, Yuan L, Cheng D. Molecular Fluorescent Probes for Liver Tumor Imaging. *Chem Asian J*. 2022;17(8):e202200091. doi:10.1002/asia.202200091
9. Schwenck J, Sonanini D, Cotton JM, et al. Advances in PET imaging of cancer. *Nat Rev Cancer*. 2023;23(7):474–490. doi:10.1038/s41568-023-00576-4
10. Li S, Li Q, Chen W, et al. A Renal-Clearable Activatable Molecular Probe for Fluoro-Photacoustic and Radioactive Imaging of Cancer Biomarkers. *Small*. 2022;18(28):e2201334. doi:10.1002/smll.202201334
11. Yuan M, Wu Y, Zhao C, et al. Activated molecular probes for enzyme recognition and detection. *Theranostics*. 2022;12(3):1459–1485. doi:10.7150/thno.66676
12. NCBI. Molecular Imaging, How Close to Clinical Precision Medicine in Lung, Brain, Prostate and Breast Cancers - PubMed. Available from: https://pubmed.ncbi.nlm.nih.gov/34269972/. Accessed December 6, 2024.
13. Jiang J, Wang S, Chen Y, Wang C, Qu C, Liu Y. Immunohistochemical characterization of lymphangiogenesis-related biomarkers in primary and recurrent gliomas: a STROBE compliant article. *Medicine*. 2018;97(39):e12458. doi:10.1097/MD.0000000000012458
14. Grau SJ, Trillsch F, Tonn JC, et al. Podoplanin increases migration and angiogenesis in malignant glioma. *Int J Clin Exp Pathol*. 2015;8 (7):8663–8670.
15. Goracci M, Pignochino Y, Marchiò S. Phage Display-Based Nanotechnology Applications in Cancer Immunotherapy. *Molecules*. 2020;25(4):843. doi:10.3390/molecules25040843
16. Takakusagi Y, Takakusagi K, Sakaguchi K, Sugawara F. Phage display technology for target determination of small-molecule therapeutics: an update. *Expert Opin Drug Discov*. 2020;15(10):1199–1211. doi:10.1080/17460441.2020.1790523
17. Saw PE, Song EW. Phage display screening of therapeutic peptide for cancer targeting and therapy. *Protein Cell*. 2019;10(11):787–807. doi:10.1007/s13238-019-0639-7
18. Li F, Zhang Z, Cai J, et al. Primary Preclinical and Clinical Evaluation of 68Ga-DOTA-TMVP1 as a Novel VEGFR-3 PET Imaging Radiotracer in Gynecological Cancer. *Clin Cancer Res*. 2020;26(6):1318–1326. doi:10.1158/1078-0432.CCR-19-1845
19. Wang X, Dai G, Jiang G, et al. A TMVP1-modified near-infrared nanoprobe: molecular imaging for tumor metastasis in sentinel lymph node and targeted enhanced photothermal therapy. *J Nanobiotechnology*. 2023;21(1):130. doi:10.1186/s12951-023-01883-6
20. Zou Y, Wang Y, Xu S, et al. Brain Co-Delivery of Temozolomide and Cisplatin for Combinatorial Glioblastoma Chemotherapy. *Adv Mater*. 2022;34 (33):e2203958. doi:10.1002/adma.202203958

21. Kundu M, Das S, Nandi S, Dhara D, Mandal M. Magnolol and Temozolomide exhibit a synergistic anti-glioma activity through MGMT inhibition. *Biochim Biophys Acta Mol Basis Dis*. 2023;1869(7):166782. doi:10.1016/j.bbadis.2023.166782
22. Aldoghachi AF, Aldoghachi AF, Breyne K, Ling KH, Cheah PS. Recent Advances in the Therapeutic Strategies of Glioblastoma Multiforme. *Neuroscience*. 2022;491:240–270. doi:10.1016/j.neuroscience.2022.03.030
23. Jia JL, Alshamsan B, Ng TL. Temozolomide Chronotherapy in Glioma: a Systematic Review. *Curr Oncol*. 2023;30(2):1893–1902. doi:10.3390/curroncol30020147
24. Fan W, Wang D, Li G, et al. A novel chemokine-based signature for prediction of prognosis and therapeutic response in glioma. *CNS Neurosci Ther*. 2022;28(12):2090–2103. doi:10.1111/cns.13944
25. Yang Z, Gong W, Zhang T, Gao H. Molecular Features of Glioma Determined and Validated Using Combined TCGA and GTEx Data Analyses. *Front Oncol*. 2021;11:729137. doi:10.3389/fonc.2021.729137
26. Witthayanuwat S, Pesee M, Supaadirek C, Supakalin N, Thamronganantasakul K, Krusun S. Survival Analysis of Glioblastoma Multiforme. *Asian Pac J Cancer Prev*. 2018;19(9):2613–2617. doi:10.22034/APJCP.2018.19.9.2613
27. Deighton RF, McGregor R, Kemp J, McCulloch J, Whittle IR. Glioma pathophysiology: insights emerging from proteomics. *Brain Pathol*. 2010;20(4):691–703. doi:10.1111/j.1750-3639.2010.00376.x
28. Lee JY, Park S, Han AR, Hwang HS, Kim HJ. Therapeutic potential of FLT4-targeting peptide in acute myeloid leukemia. *Cancer Immunol Immunother*. 2023;72(9):2919–2925. doi:10.1007/s00262-023-03385-8
29. Vincent MP, Stack T, Vahabikashi A, et al. Surface Engineering of FLT4-Targeted Nanocarriers Enhances Cell-Softening Glaucoma Therapy. *ACS Appl. Mater. Interfaces*. 2021;13(28):32823–32836. doi:10.1021/acsami.1c09294
30. Kao TJ, Lin CL, Yang WB, Li HY, Hsu TI. Dysregulated lipid metabolism in TMZ-resistant glioblastoma: pathways, proteins, metabolites and therapeutic opportunities. *Lipids Health Dis*. 2023;22(1):114. doi:10.1186/s12944-023-01881-5
31. Wang G, Wang W. Advanced Cell Therapies for Glioblastoma. *Front Immunol*. 2022;13:904133. doi:10.3389/fimmu.2022.904133
32. Kumar VR, Kampan NC, Abd Aziz NH, Teik CK, Shafiee MN, Menon PS. Recent Advances in Surface Plasmon Resonance (SPR) Technology for Detecting Ovarian Cancer Biomarkers. *Cancers*. 2023;15(23):5607. doi:10.3390/cancers15235607
33. Nguyen HH, Park J, Kang S, Kim M. Surface plasmon resonance: a versatile technique for biosensor applications. *Sensors*. 2015;15(5):10481–10510. doi:10.3390/s150510481
34. Li CM, Haratipour P, Lingeman RG, et al. Novel Peptide Therapeutic Approaches for Cancer Treatment. *Cells*. 2021;10(11):2908. doi:10.3390/cells10112908
35. Alas M, Saghaeidehkordi A, Kaur K. Peptide-Drug Conjugates with Different Linkers for Cancer Therapy. *J Med Chem*. 2021;64(1):216–232. doi:10.1021/acs.jmedchem.0c01530
36. Kalmouni M, Al-Hosani S, Magzoub M. Cancer targeting peptides. *Cell mol Life Sci*. 2019;76(11):2171–2183. doi:10.1007/s00018-019-03061-0
37. Pisani S, Di Martino D, Cerri S, et al. Investigation and Comparison of Active and Passive Encapsulation Methods for Loading Proteins into Liposomes. *Int J mol Sci*. 2023;24(17):13542. doi:10.3390/ijms241713542
38. Javid H, Oryani MA, Rezagholinejad N, Esparham A, Tajaldini M, Karimi-Shahri M. RGD peptide in cancer targeting: benefits, challenges, solutions, and possible integrin-RGD interactions. *Cancer Med*. 2024;13(2):e6800. doi:10.1002/cam4.6800
39. Cossu J, Thoreau F, Boturyn D. Multimeric RGD-Based Strategies for Selective Drug Delivery to Tumor Tissues. *Pharmaceutics*. 2023;15(2):525. doi:10.3390/pharmaceutics15020525
40. Xie J, Shen Z, Anraku Y, Kataoka K, Chen X. Nanomaterial-based blood-brain-barrier (BBB) crossing strategies. *Biomaterials*. 2019;224:119491. doi:10.1016/j.biomaterials.2019.119491
41. Zhao Y, Gan L, Ren L, Lin Y, Ma C, Lin X. Factors influencing the blood-brain barrier permeability. *Brain Res*. 2022;1788:147937. doi:10.1016/j.brainres.2022.147937
42. Sm L, S M, Ae T. Key for crossing the BBB with nanoparticles: the rational design. *Beilstein J Nanotechnol*. 2020;11:72. doi:10.3762/bjnano.11.72
43. Chen W, Wang D, Du X, et al. Glioma cells escaped from cytotoxicity of temozolomide and vincristine by communicating with human astrocytes. *Med Oncol*. 2015;32(3):43. doi:10.1007/s12032-015-0487-0
44. Feng SW, Chang PC, Chen HY, Hueng DY, Li YF, Huang SM. Exploring the Mechanism of Adjuvant Treatment of Glioblastoma Using Temozolomide and Metformin. *Int J mol Sci*. 2022;23(15):8171. doi:10.3390/ijms23158171
45. Choo M, Mai VH, Kim HS, et al. Involvement of cell shape and lipid metabolism in glioblastoma resistance to temozolomide. *Acta Pharmacol Sin*. 2023;44(3):670–679. doi:10.1038/s41401-022-00984-6
46. Shah S, Dhawan V, Holm R, Nagarsenker MS, Perrie Y. Liposomes: advancements and innovation in the manufacturing process. *Adv Drug Deliv Rev*. 2020;154-155:102–122. doi:10.1016/j.addr.2020.07.002
47. Lamichhane N, Udayakumar TS, D'Souza WD, et al. Liposomes: clinical Applications and Potential for Image-Guided Drug Delivery. *Molecules*. 2018;23(2):288. doi:10.3390/molecules23020288